Enzymatic Activity Profiling Using an Ultra-Sensitive Array of Chemiluminescent Probes for Bacterial Classification and Characterization

Shelef, Omri;[a†] Kopp, Tal;[a†] Tannous, Rozan;[a†] Arutkin, Maxence;[a] Jospe-Kaufman, Moriah;[a] Reuveni, Shlomi;[a*] Shabat, Doron [a*] and Fridman, Micha [a*].

[a]School of Chemistry, Raymond & Beverly Sackler Faculty of Exact Sciences, Tel Aviv University, Tel Aviv, 6997801, Israel.

[†]These authors contributed equally to this study.

*Correspondence to: Shlomi Reuveni, shlomire@tauex.tau.ac.il; Doron Shabat, chdoron@tauex.tau.ac.il; Micha Fridman, mfridman@tauex.tau.ac.il.

ABSTRACT

Bacterial species identification and characterization in clinical and industrial settings necessitate the use of diverse, labor-intensive, and time-consuming protocols, as well as the utilization of expensive and high-maintenance equipment. Furthermore, while cutting-edge identification technologies like mass spectrometry and PCR are highly effective in identifying bacterial pathogens, they fall short in providing crucial information for identifying bacteria not present in the databases upon which these methods rely. In response to these challenges, we present a robust and general approach to bacterial identification, based on their unique enzymatic activity profiles. This method delivers results within 90 minutes, utilizing an array of highly sensitive and enzyme-selective chemiluminescent probes. Leveraging our recently developed technology of chemiluminescent luminophores, which emit light under physiological conditions, we have crafted an array of probes designed to rapidly detect various bacterial hydrolytic enzymatic activities, including some associated with antibiotic resistance. The analysis of chemiluminescent fingerprints from a diverse range of prominent bacterial pathogens has unveiled distinct enzymatic activity profiles for each strain. The reported universally applicable identification procedure offers a highly sensitive and expeditious means to delineate bacterial enzymatic activity profiles. This breakthrough opens new avenues for characterizing and identifying pathogens in research, clinical, and industrial applications.

INTRODUCTION

Accurately identifying microorganisms and comprehensively characterizing their diverse attributes in a dependable, rapid, and cost-effective manner presents a substantial challenge[1]. Rapid and precise identification and characterization of pathogens are crucial to ensure accurate diagnosis, effective treatment, and the prevention of outbreaks in clinical, industrial, and agricultural settings[2].

Clinical microbiology laboratories endeavor to attain precise bacterial identification and determine drug susceptibility profiles[3,4]. This empowers physicians to make informed decisions swiftly regarding optimal treatment options[5,6]. The progression of the COVID-19 pandemic has highlighted the pivotal role of research and clinical microbiology laboratories in uncovering the sources and modes of transmission of outbreaks. This essential information is paramount for effectively controlling infectious diseases and averting their widespread dissemination and recurrence.

In recent decades, the field of pathogen identification has experienced significant advancement through the introduction of innovative analytical methods reliant on modern technologies and equipment[7]. Among these advancements, next-generation sequencing has transformed microbial diagnostics by enabling unbiased and hypothesis-free detection of a wide spectrum of microbial pathogens, both common and rare, without the necessity for prior culture growth[8]. Another method gaining increasing prominence in clinical microbiology laboratories is mass spectrometry-based techniques, with a particular focus on matrix-assisted laser desorption/ionization time-of-flight mass spectrometry (MALDI-TOF MS)[9]. This method has demonstrated its effectiveness in identifying pathogenic bacteria, including micro-aerobes, anaerobes, mycobacteria, and fungi[10]. Its extensive and robust database, coupled with exceptional performance, guarantees rapid and precise outcomes, without the necessity for highly specialized laboratory personnel to oversee the procedure. Nonetheless, it's worth noting that this technology has limitations; it can solely identify isolates if the measured spectrum contains peptide mass fingerprints of the pathogen found in a given database, which can diminish its effectiveness when dealing with newly emerging pathogens[11]. It's also important to highlight that molecular microbiology methods like 16S sequencing and MALDI-TOF do not offer insights into

specific pathogenic strain properties, such as drug resistance or virulence levels[12]. Lastly, the widespread adoption of sequencing and mass spectrometry technologies faces obstacles due to their substantial instrumentation costs and infrastructure requirements. These requirements include a stable power supply, maintenance by qualified technicians, a dust-free environment, and a stable climate[13,14]. As a result, a significant percentage of the world's population still faces barriers to accessing these advanced technologies.

Traditional practices, such as assessing Gram stain and colony morphology, utilizing acid-fast stains, and conducting spot indole oxidase tests, continue to be widely used around the globe[7,15]. Nonetheless, owing to the immense diversity of the microbiome and the evolving comprehension of microbiological pathogenicity, these methods frequently lack the precision needed for definitive pathogen identification[16]. Conventional identification processes, following streaking procedures, are time-consuming, spanning from hours to days, contingent upon the type of pathogen involved[17]. As an illustration, diagnosing infectious diarrhea via bacterial culture and identification in stool samples usually demands 3–5 days, rendering it a complex and expensive procedure with limited applicability for point-of-care treatments[18].

To tackle these challenges, numerous clinical microbiology labs have adopted FDA or EMA-approved biochemical kits, i.e., the Analytical Profile Index (API), for the identification of bacterial pathogens[19]. These kits entail a series of complementary tests conducted sequentially, guided by a flowchart-based identification procedure. The API identification process initiates with Gram staining, an oxidase test, and a fermentation test. Depending on the initial findings, the appropriate API kit is chosen for the ultimate identification and categorization of the pathogen. As an example, in the API 20E kit, a plastic strip featuring twenty mini-test chambers containing dehydrated media is utilized, with specific probes employed for each mini-test[20,21]. The metabolic activities of the introduced organisms, including processes like carbohydrate fermentation or protein catabolism, trigger color changes during incubation. These color changes are subsequently matched with profile numbers in a commercial codebook (or online resource) to ascertain bacterial species identification. This colorimetric identification process

usually necessitates an incubation period of 18–24 hours, although certain tests may extend beyond this timeframe[19,21]. Another widely employed method for identifying microbial pathogens involves assessing carbon-source utilization profiles[22,23]. In this approach, a kit featuring a 96-well plate containing diverse carbon sources is utilized. Like the API method, carbon source profiling is time-consuming, owing to the essential incubation period for obtaining discernible results and the necessity of choosing the suitable growth conditions for the unidentified bacterial pathogen within the sample.

To address the challenges of existing identification methodologies, researchers around the world, including ourselves, have developed a remarkably sensitive and expeditious method for classifying and characterizing bacterial pathogens using chemiluminescent agents[24-27]. In contrast to fluorescence, chemiluminescence presents distinct advantages, including the absence of the need for external light irradiation. This characteristic leads to an exceptionally minimal background signal and heightened sensitivity, setting it apart from fluorescence-based and colorimetric assays[28,29].

A fascinating category of chemiluminescent compounds, referred to as triggerable phenoxy-dioxetanes, has drawn specific attention (Figure 1A)[30,31]. This feature enables the linkage of light emission to the actions of specific analytes by including a suitable phenol-protecting group as a triggering substrate. Nevertheless, despite their promise, the limited emission intensity of these dioxetane compounds in aqueous solutions has rendered them unsuitable for utilization in biological assays conducted in such settings[32]. To overcome this foundational hurdle, one of our groups has recently achieved a significant breakthrough. It was found that incorporating an acrylate substituent at the *ortho* position of a phenoxy-adamantyl-1,2-dioxetane diminishes the water-quenching effect on the excited benzoate intermediate (Figure 1B)[33]. Furthermore, this alteration enhances the light-emission intensity of the chemiluminescence luminophore by up to three orders of magnitude in comparison to the original phenoxy-dioxetanes (Figure 1C). This pivotal advancement has empowered researchers to employ chemiluminescence probes in aqueous solutions without the necessity for additives, thereby broadening their scope for potential applications in biological studies[34-43].

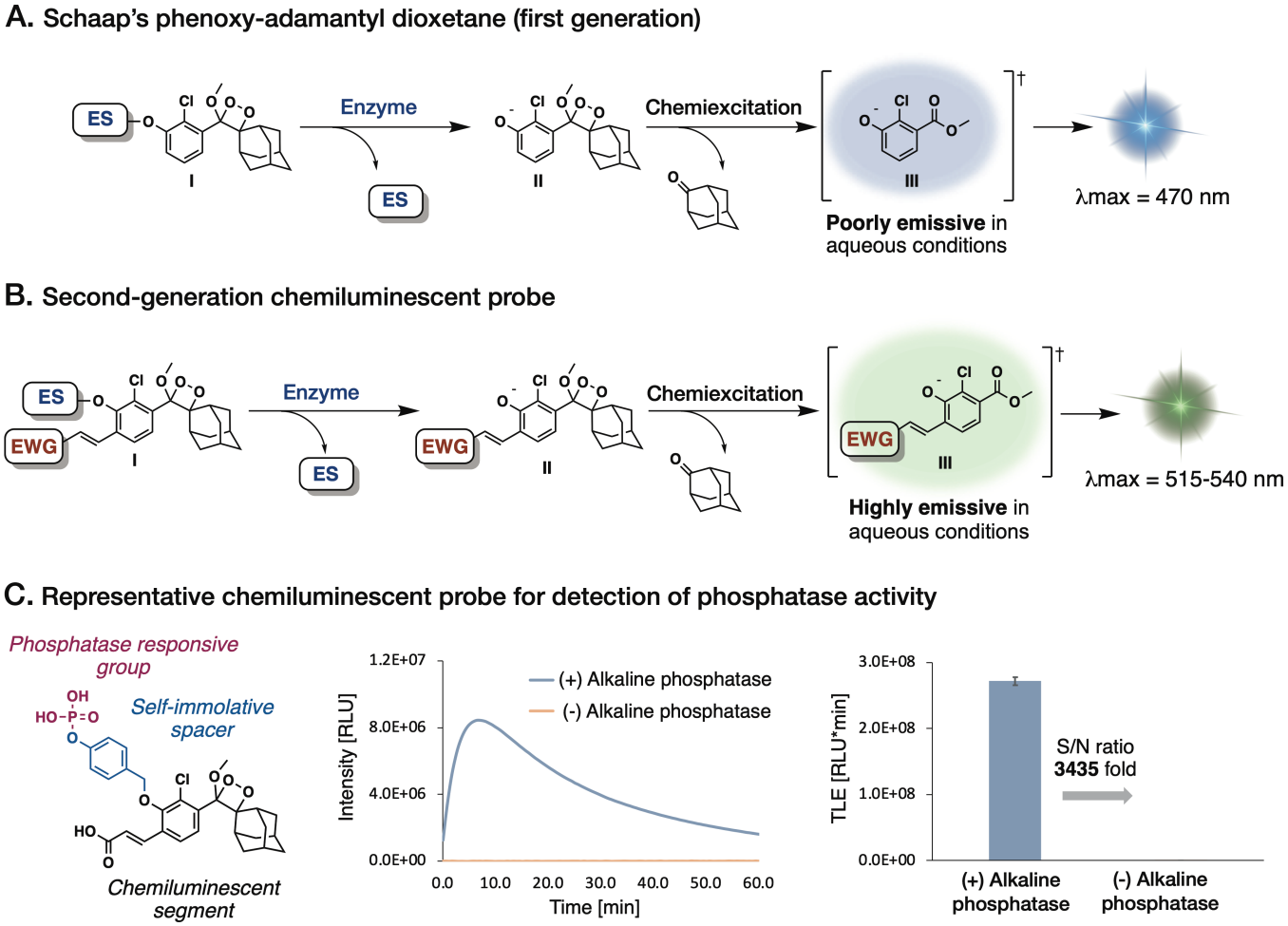

Figure 1. Structures and chemiexcitation pathways of **(A)** Schaap's dioxetane-based probes, and **(B)** ortho-substituted phenoxy 1,2-dioxetane probes. **(C)** Representative chemical structure, chemiluminescent kinetic profile, and total light emitted (TLE) during one hour by phosphatase-triggered chemiluminescent probe [10 □M] with or without commercial alkaline phosphatase [1 U/mL] in PBS pH 7.4, 0.1% DMSO, 37°C. (ES, enzymatic substrate; EWG, electron-withdrawing group; S/N, signal to noise).

In this study, we present a novel and general approach for rapid classification and identification of bacterial pathogens. Our innovative method harnesses the power of ultra-sensitive chemiluminescent probes to create unique enzymatic activity fingerprints. These fingerprints serve as an exceptionally effective tool for quickly and accurately characterizing and identifying various bacterial pathogens, as well as for providing important information on the enzymatic activity profiles that can be used to identify bacteria even if they are not in the database.

RESULTS AND DISCUSSION

Chemiluminescent probes outperform in signal-to-noise ratio and limit-of-detection compared to fluorescent and colorimetric probes. To explore the advantages of developing an array of chemiluminescent probes in comparison to fluorescent or colorimetric probes, we evaluated three related probes for their ability to detect specific enzymatic activity. In each of these probes, the same phosphatase-triggering substrate initiates specific light-emitting reactions. These reactions activate one of three optical signaling mechanisms: *ortho* acrylate-substituted phenoxy-adamantyl-1,2-dioxetane (for chemiluminescence), 7-hydroxy-coumarin (for fluorescence), or a *para*-nitrophenol dye (for colorimetry) (Figure 2A)[44]. Upon interaction with the phosphatase enzyme, the cleavable phosphate headgroup substrate a phenolate functional group is formed. This is followed by a subsequent disassembly phase characterized by a 1,6-elimination reaction, leading to the liberation of a quinone-methide molecule. Concurrently, this reaction triggers the emission of the respective optical signal, whether it be chemiluminescent, fluorescent, or colorimetric, as part of the reporting mechanism.

Activation of the probes with recombinant alkaline phosphatase revealed that the phosphatase limit-of-detection (L.O.D) value of the chemiluminescent probe was ~25-fold lower than that of the fluorescent probe which was in turn ~125-fold lower than that of the colorimetric probe (Figure 2B and Figures S1-S6). We next compared the performance of the three optical probes in the presence of bacteria. Phosphatase activity was measured while incubating each of the three probes in PBS, pH=7.4 buffer containing cells of *Staphylococcus aureus* (ATCC 29213). The L.O.D value for the chemiluminescent probe was ~25-fold lower than that of the fluorescent probe which was in turn ~25-fold lower than that of the colorimetric probe (Figure 2C and Figures S7-S9). Moreover, the signal-to-noise ratio of the chemiluminescent probe was ~70-fold higher than that of the fluorescent probe and ~673-fold higher than that of the colorimetric probe; hence, chemiluminescence detection based on a phenoxy-adamantyl-1,2-dioxetane unit was chosen as the superior detection method for the designed array of enzymatic activity sensors (Figure 2C and Figures S7-S9).

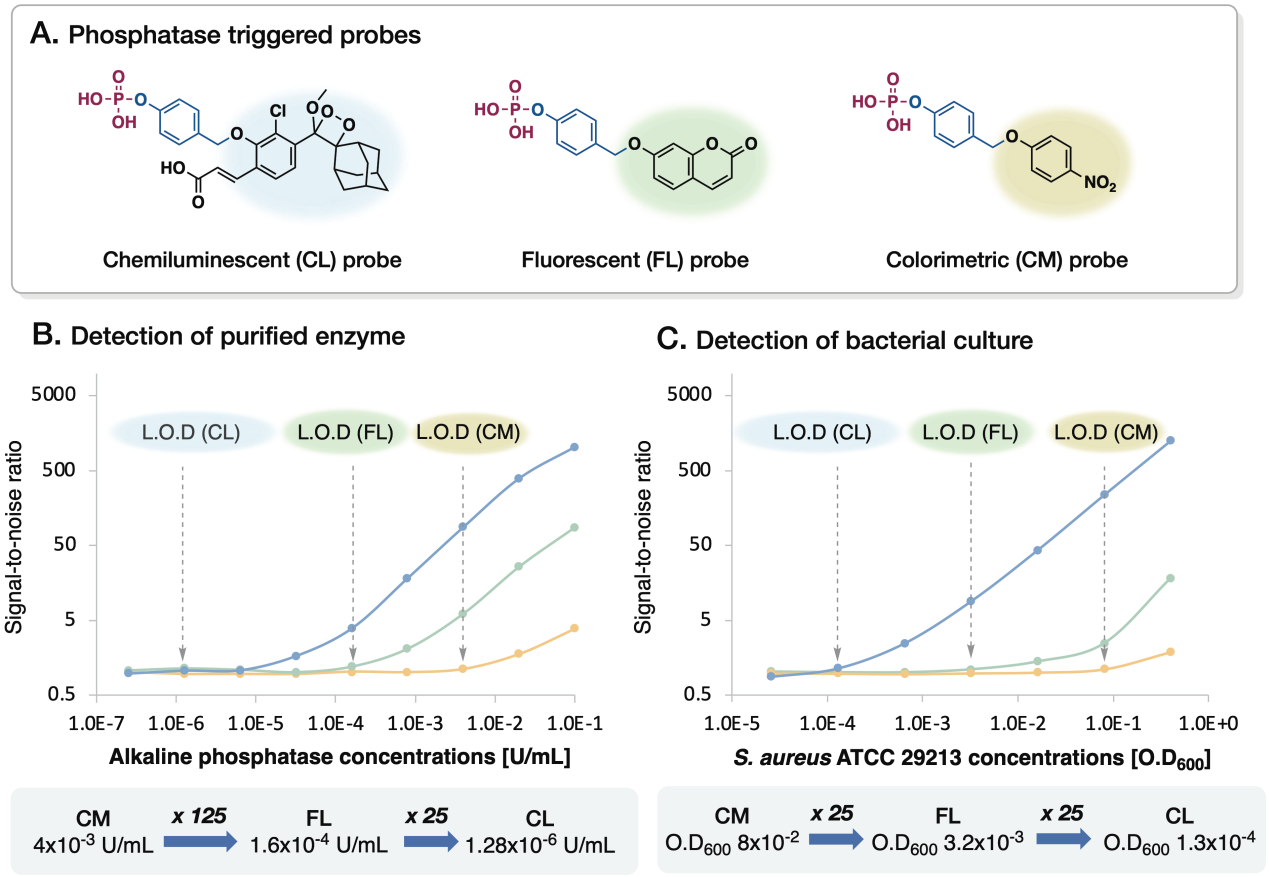

Figure 2. Comparison between the limit of detection of phosphatase-triggered probes. **(A)** structure of chemiluminescent [10 □M], fluorescent [10 □M], and colorimetric [100 □M] phosphatase probes. Limit of detection in the presence of a 5-fold serial dilution of **(B)** commercial alkaline phosphatase [0.1 - 2.56 x10^{-7} U/mL] and **(C)** *S. aureus* ATCC 29213 [0.4 - 2.56x10^{-5} O.D_{600}], in PBS pH 7.4, 0.1% DMSO, 37°C. (CL, chemiluminescent; FL, fluorescent; CM, colorimetric, L.O.D, limit of detection).

Design and synthesis of an array of highly stable chemiluminescent probes for sensing catabolic bacterial enzymes with high substrate specificity. Taking advantage of the chemiluminescent phosphatase probe's heightened sensitivity, we constructed an array comprised of 12 chemiluminescent probes (depicted in Figure 3A, full synthesis presented in Scheme S1-S10). This array consists of 10 distinct triggers, each representing a substrate of a different prevalent bacterial enzymatic activity[45-47]. We also included two control probes: an N-acetyl hydrolase probe for non-specific N-deacetylase detection and a periodate oxidative-cleavage probe. The periodate oxidative-cleavage probe is unresponsive to bacterial activation and served as a negative control.

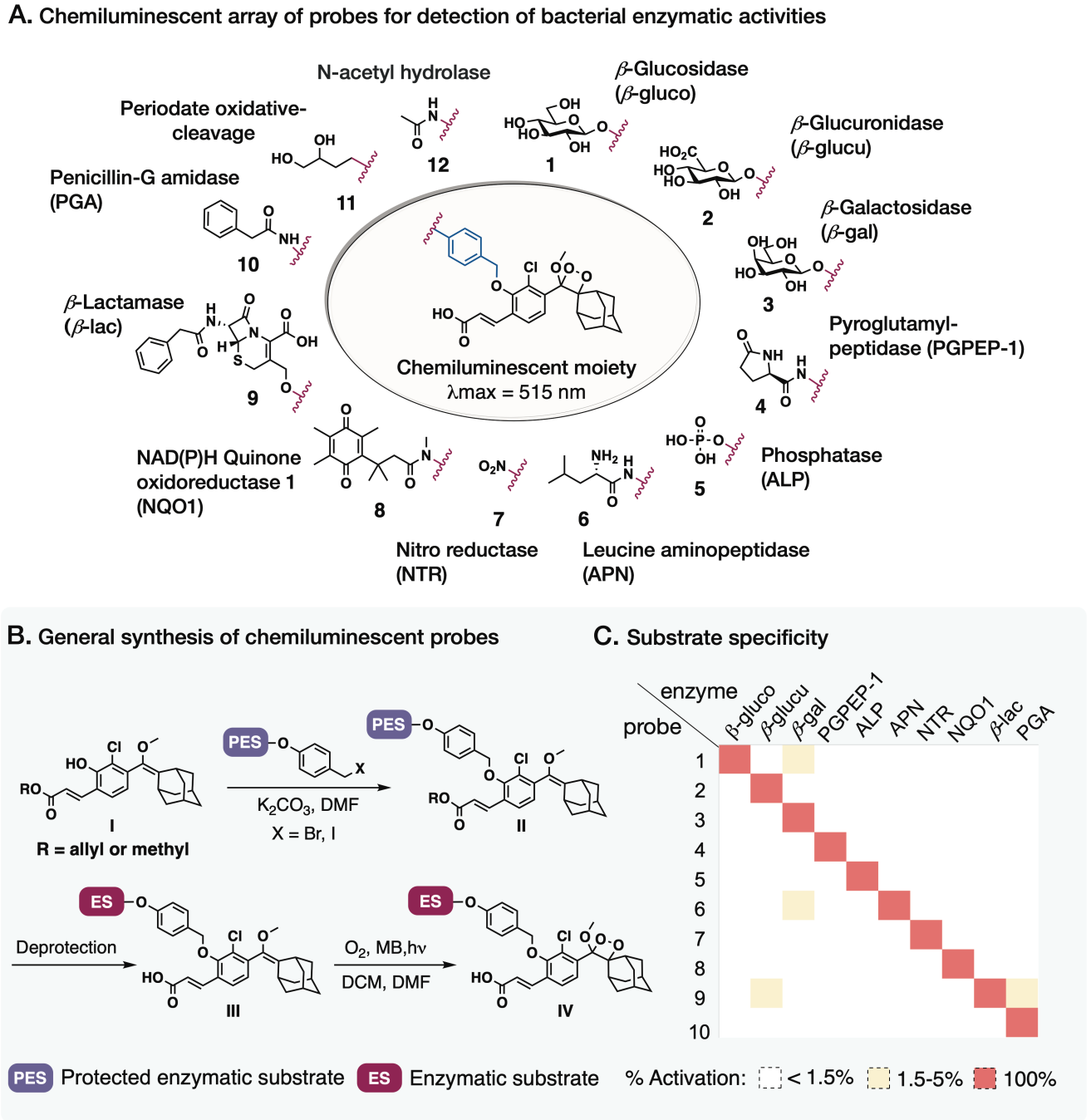

Figure 3. Synthesis and substrate specificity evaluation of the array of chemiluminescent probes. (**A**) Structures of the 12 chemiluminescent probes comprising the array; (**B**) General synthetic pathways for the preparation of chemiluminescent probes; (**C**) Substrate specificity evaluation of 10 probes [10 □M] in the presence of 10 commercially available enzymes (β-glucosidase [10 U/mL], β-glucuronidase [1 U/mL], β-galactosidase [1 U/mL], Pyroglutamyl-peptidase I [0.05 mg/mL], Alkaline phosphatase [1 U/mL], Aminopeptidase-M [1 U/mL], Nitroreductase [1 mg/mL, 100mM], NAD(P)H quinone oxidoreductase [0.8 mg/mL, 100mM NADH], β-Lactamase [2 U/mL], Penicillin-G amidase [1 U/mL].

We proceeded to investigate the chemiluminescent probes' specificity as substrates for the target enzymes, assessing them across a panel of recombinant enzymes corresponding to the 10 sensed activities (depicted in Figure 3C, and Figures S10-S25). The probes within the array exhibited favorable selectivity as substrates for their designated enzymes with mild background for some of the probes (Figure 3C). Finally, to assess the probes' stability within the array, we examined their behavior under assay conditions (PBS [100mM], pH 7.4, 0.1% DMSO, 37°C, 60 min). The probes demonstrated satisfactory stability, with the β-lactamase probe exhibiting the least stability (~1% decomposition) and the β-galactosidase probe showcasing remarkable stability, with decomposition of less than 0.00001%. Additionally, DMSO stock solutions of the probes stored at -20°C remained unchanged for over a year.

The array of chemiluminescent probes yields distinct enzymatic activity profiles, enabling differentiation between different species of bacteria. Employing the 12-probe chemiluminescent array, we characterized enzymatic activity profiles across a panel encompassing 25 strains representing 15 distinct Gram-positive and Gram-negative species (Table S1). This panel included prominent bacterial pathogens and members of the ESKAPE group[48]. The streamlined process, taking approximately 1.5 hours to complete, is outlined in Figure 4A. This refined procedure consistently yielded reproducible enzymatic activity profiles for each strain, culminating in a comprehensive database comprising 12-dimensional vectors that encapsulate the total emitted light. We assessed the logarithm of the ratio between the total emitted light and the background light, which we have identified as a background-subtracted proxy for enzymatic activity. Each strain displayed a distinct enzymatic activity fingerprint based on this metric, underscoring the array's potential for bacterial species classification and even strain differentiation. Chemiluminescent kinetic profiles and total light emission (TLE) profiles of four representative bacteria are presented in Figures S26-S31, complete light emission profiles of the bacteria are presented in Figures S32-S34, and PCA species analysis results in Figures S35-S37.

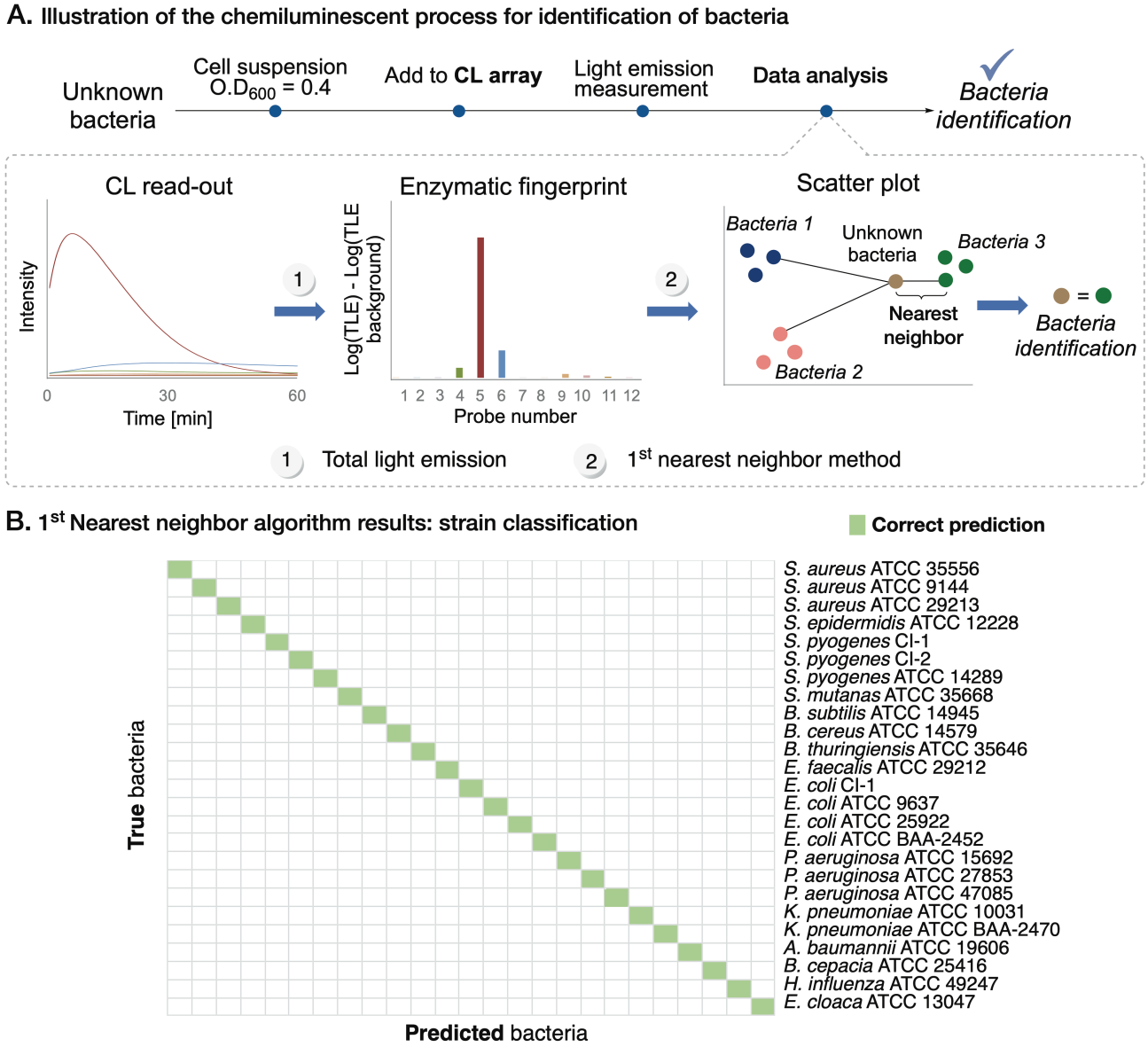

Figure 4. Profiling bacterial enzymatic activities with chemiluminescent probes. **(A)** Schematic representation of the bacterial identification process, which can be completed in 1.5 hours. **(B)** Application of the 1-N-N method to analyze the database, successfully distinguishing between all 25 strains in the panel. Detailed assay procedures are described in the supporting information. (TLE, total light emission; CI, clinical isolate)

The analysis of the resulting database was conducted utilizing the first nearest-neighbor method (1-N-N) predicated on enzymatic activity (log-ratios) within the data space (depicted in Figure 4A)[49]. This proposed methodology offers a direct and efficient means for bacterial identification through the scrutiny of chemiluminescent probe data. Employing the 1-N-N analysis on the 12-probe enzymatic activity

fingerprint yielded distinct differentiation among all 25 diverse bacterial strains encompassing our panel (Figure 4B and Figures S38-S39).

To determine whether fewer probes could achieve comparable accuracy, we examined the variance in each probe's response across all the bacterial strains in our panel (Figure S40). Interestingly, selecting the five most variable probes (5, 4, 2, 7, and 6) was sufficient to distinguish all 25 diverse bacterial strains in our panel. We also explored the impact of assay duration on species identification accuracy. A 15-minute chemiluminescence (CL) measurement yielded an accuracy of 82%. Extending the measurement to 30- and 45-minutes improved accuracy to 92% and 96%, respectively. These findings highlight the significant potential of enzymatic activity footprint analysis as a reliable and efficient tool for bacterial identification. Of note, performing the commercial API method on two different bacterial species revealed similar identification results to our approach. However, separate API kits were required for each bacterial species, and the identification was limited to the species level. Additionally, the API-based assay took 24 hours to complete. In contrast, our approach enables universal strain-level identification within a brief 90-minute timeframe (Figures S41-S43).

Through comparative analyses of the specific probe's TLE across the various bacteria in the panel, several unexpected discoveries emerged. Notably, when examining the mean β-glucuronidase activity across all *E. coli* strains in the panel, a significantly higher value was observed compared to other bacteria (as demonstrated in Figure 5A and Figure S44). This elevated activity facilitated the differentiation of *E. coli* strains within the panel solely based on β-glucuronidase activity alone. This aligns with prior reports that designate β-glucuronidase as a marker for *E. coli* presence[46]. Harking back to the mid-1970s, Kilian and Bulow scrutinized clinical *E. coli* isolates, discovering that around 97% exhibit β-glucuronidase production, while the majority of other coliform bacteria do not[50]. A total of 460 humans, 105 cows, and 55 horses *E. coli* isolates were tested. Results showed 95.5% *β*-glucuronidase-positive isolates in 24 h and 99.5% positive after 28 h of incubation.

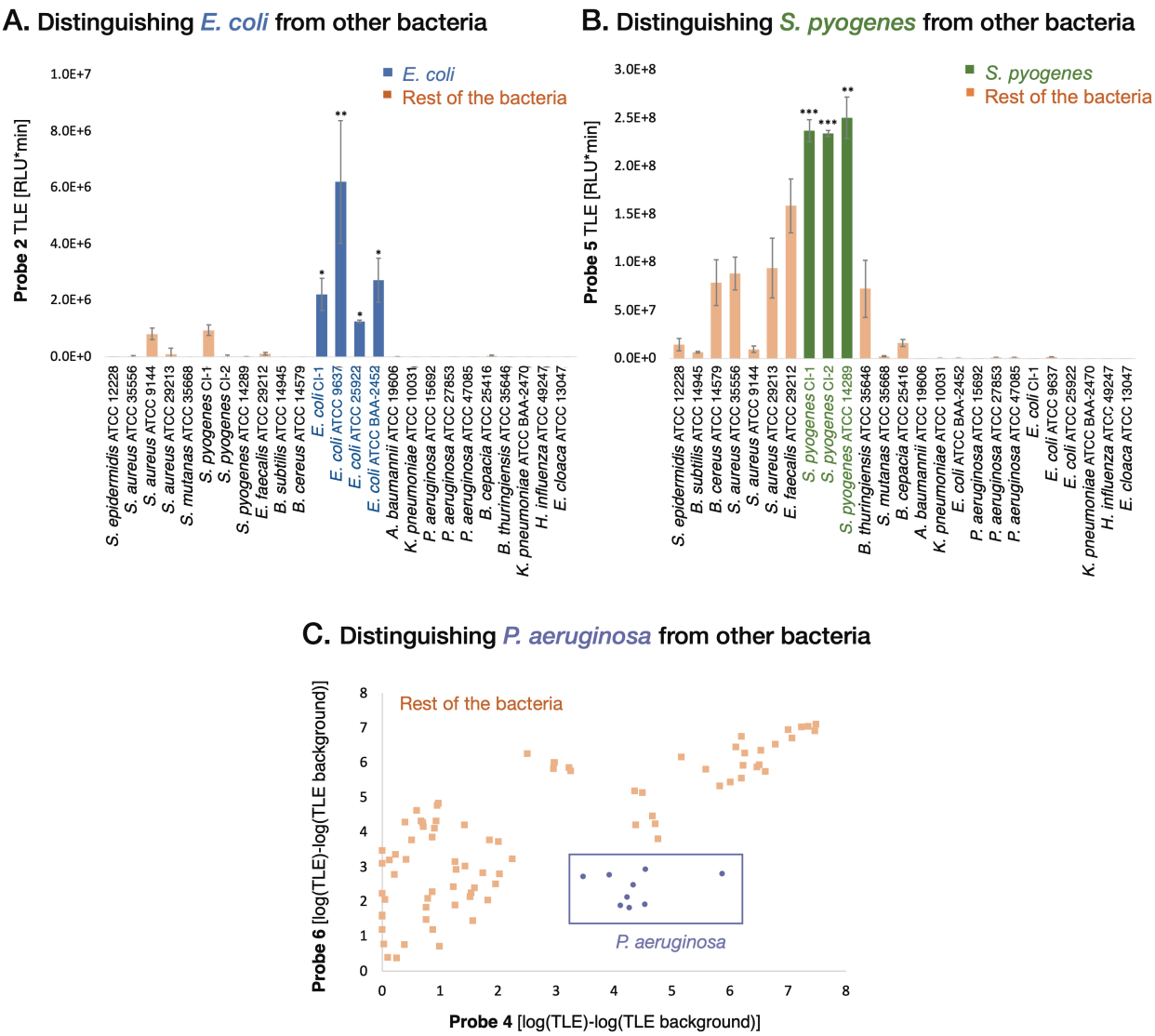

Figure 5: Several species in the panel can be identified based on the high activity of one or two of the chemiluminescent enzyme probes in the array. **(A)** TLE by the β-glucuronidase probe 2; **(B)** TLE by the phosphatase probe 5; **(C)** presents a scatter plot of the TLE by the pyroglutamyl peptidase probe 4 and leucine aminopeptidase probe 6 from the 25 strains of bacteria.

Similarly, the TLE of the phosphatase probe 5, was significantly higher for the *S. pyogenes* strains in the panel than for all other strains (Figure 5B and Figure S45). *S. pyogenes*, also known as Group A *Streptococcus*, is a group of Gram-positive bacteria which can be carried in human throats or skin, and it is responsible for more than 500,000 deaths worldwide annually[51].The conventional tests for identification of *S. pyogenes* in clinical samples involve blood agar plates that are screened for the

presence of β-hemolytic colonies[52]. The typical appearance of *S. pyogenes* colonies after 24 hours of incubation at 35-37°C is dome-shaped with a smooth or moist surface and clear margins. Importantly, automated bacterial identification by MALDI-TOF has limitations in identifying several streptococcal species (including *S. dysgalactiae* subsp. *equisimilis,* which may be misidentified as *S. pyogenes*)[53]. Several point-of-care tests for the detection of *S. pyogenes* in throat swabs using rapid automated PCR technology have received FDA clearance to date, yet the use of PCR for diagnosing streptococcal throat infections remains low[54]. Our method suggests that testing for high levels of phosphatase could potentially provide an affordable substitute for the detection of *S. pyogenes*.

Pseudomonas aeruginosa is yet another bacterium which can be easily identified using our method. Prior studies have indicated that *Pseudomonas aeruginosa* exhibits pyroglutamyl aminopeptidase activity[55]. Interestingly, using solely the pyroglutamyl aminopeptidase probe yielded a success rate of 92% in distinguishing *Pseudomonas aeruginosa* strains from all other bacteria within our panel. Moreover, a dual-probe strategy involving pyroglutamyl aminopeptidase and leucine aminopeptidase achieved 100% identification accuracy (as illustrated in Figure 5C and Figure S46).

Subsequently, we delved into the potential of the chemiluminescence-based enzymatic profiling method for categorizing bacteria not originally included in the original database. We employed a chi-squared (χ^2) metric to quantify the resemblance between bacteria not originally included in the database. Specifically, we focused on three bacterial strains: *Staphylococcus aureus* ATCC 33591, an *Escherichia coli* clinical isolate, and a clinical isolate of *Pseudomonas aeruginosa*. To assess their similarity to known strains, we adopted a statistical approach, which involved representing each strain in the original data set as a Gaussian cloud within the 12-dimensional space corresponding to log-ratios of the TLE from each probe. This representation allowed us to rank the similarity of new bacteria to existing strains in our data set and statistically test the hypothesis that they are one and the same.

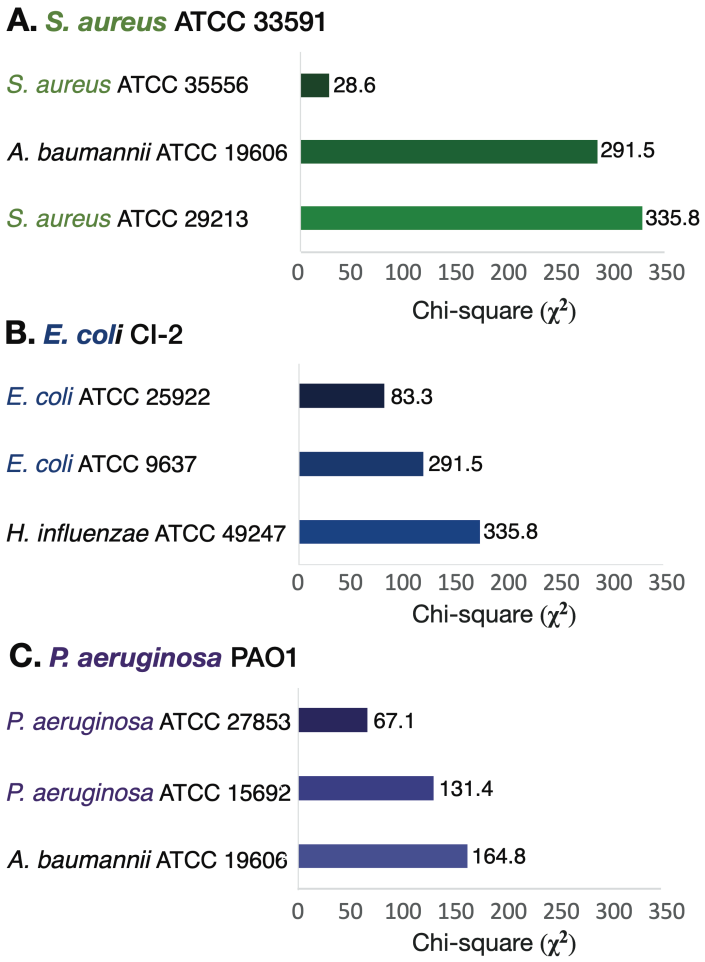

Figure 6. Top three most similar strains for three unknown bacteria that were not included in the initial panel; **(A)** *S. aureus* ATCC 33591 classified with the highest resemblance as *S. aureus*, **(B)** *E. coli* clinical isolate-2 (CI-2) classified with the highest resemblance as *E. coli, and* **(C)** *P. aeruginosa* PAO1 classified with the highest resemblance as *P. aeruginosa.*

Using the χ^2 metric, we conducted a thorough comparison of the enzymatic profiles of the selected strains with those in our panel. The results of this analysis are summarized in Figure 6. Notably, the statistical findings consistently demonstrated that all three examined bacteria exhibit the highest resemblance to known panel bacteria from the same species. It is important to emphasize that in all cases, the p-values resulting from the χ^2 test indicated a rejection of the hypothesis that the unknown bacteria were present in the database. Instead, our analysis consistently highlighted the closest strains from the same bacterial families as the most resembling. For instance, *S. aureus* ATCC 33591 showed

the highest resemblance to *S. aureus* ATCC 35556, while the *E. coli* clinical isolate closely resembled *E. coli* ATCC 25922. Similarly, the enzymatic profile of the *P. aeruginosa* PAO1 demonstrated resemblance to *P. aeruginosa* ATCC 27853. These results underscore the effectiveness of the chemiluminescence-based enzymatic profiling method in categorizing and identifying unknown bacteria.

CONCLUSIONS

In summary, our study introduces a robust and cost-effective method for the identification and characterization of bacteria, addressing the challenges posed by labor-intensive protocols and expensive and hard to maintain equipment. This approach holds promise for widespread adoption in microbiology laboratories worldwide, facilitating well-informed decisions regarding bacterial contaminations. The development of a 12-probe array of highly sensitive and enzyme-selective chemiluminescent probes represents a significant advancement. It enables the rapid acquisition of bacteria's enzymatic activity fingerprints in just 90 minutes. These chemiluminescent fingerprints reveal unique enzymatic activity profiles for each tested bacterial strain, forming the basis for identifying unknown bacteria by comparison with an established database. Moreover, when encountering bacteria not present in the existing database, a comparative analysis of their enzymatic profiles provides valuable insights into potential identities, aiding in the formulation of eradication strategies. By expediting bacterial identification and characterization while offering essential information about their primary enzymatic activities, this method can also suggest potential new approaches for combination therapy using enzyme inhibitors. Overall, the characterization method reported herein marks a notable step forward in precise diagnosis, with applications in both fundamental research, clinical, and industrial applications.

METHODS

Luminescent probe synthesis was conducted involving the compounds, including chemiluminescent probes 1-6, 9-12, alongside the colorimetric and fluorescent probes for alkaline phosphatase. This study confirmed their identity through ^{1}H-NMR, ^{13}C-NMR, and ^{31}P-NMR spectra, as well as Mass spectroscopy. Furthermore, their purity was ascertained by Reverse-phase high-pressure liquid chromatography. Key reaction protocols are outlined below, while comprehensive synthetic schemes and procedures, as well as ^{1}H-NMR, ^{13}C-NMR, Mass spectroscopy spectra, and analytical HPLC chromatograms, are provided in the Supplementary Information section (Figure S48-S125).

General synthesis of the chemiluminescent probes: The conjugation of the enzymatic substrate precursor with the chemiluminescent precursor entailed a nucleophilic substitution reaction, involving a pre-synthesized phenol enol ether and either benzyl-iodide or benzyl-bromide. The procedure was conducted as follows: The phenol enol ether (0.10 mmol, 1.2 eq.) and K_2CO_3 (0.15 mmol, 1.5 eq.) were dissolved in 1 mL of DMF and stirred for 5 minutes. Subsequently, benzyl-iodide or benzyl-bromide (0.08 mmol, 1 eq.) was introduced into the solution. The reaction mixture was then stirred at room temperature and monitored via TLC, utilizing an EtOAc/Hexane mixture as the mobile phase. Once the reaction concluded, the mixture was diluted with 100 mL of EtOAc and subjected to washing with 50 mL of 0.1 M HCl and 50 mL of brine. The organic layer was separated, desiccated with Na_2SO_4, and subsequently evaporated under reduced pressure. The resulting crude product underwent purification by column chromatography on silica gel, employing an EtOAc/Hexane mixture for elution, to yield the desired conjugation product.

To achieve deprotection of the enzymatic substrate precursor, an aqueous basic environment was employed, culminating in the final enzymatic substrate. The conjugation product (0.07 mmol, 1 eq.) was dissolved in a 1 mL solution of 4:1 THF:H_2O, alongside LiOH (0.7 mmol, 10 eq.). Stirring of the reaction

mixture took place at 40 °C, and progress was tracked by RP-HPLC. After the reaction's completion, solvent concentration occurred under reduced pressure, followed by further purification through preparative RP-HPLC, utilizing a gradient of CH_3CN in water with 0.1% TFA. Fractions encompassing the desired final product were pooled and subjected to overnight freeze-drying.

For the enzymatic substrates of chemiluminescent probes 5 and 9, as well as the colorimetric and fluorescent probes for alkaline phosphatase, initial protection involved allyl-protecting groups. Consequently, deprotection was achieved through a standard allyl deprotection method. The protected probe (0.04 mmol, 1 eq.) was dissolved in 2 mL of CH_2Cl_2, accompanied by the addition of DMBA (0.13 mmol, 3 eq.) and tetrakis(triphenylphosphine)palladium (0.004 mmol, 0.1 eq.). Stirring of the reaction occurred at room temperature, and monitoring was conducted via RP-HPLC. After the deprotection process concluded, solvent concentration under reduced pressure transpired, followed by purification through preparative RP-HPLC using a CH_3CN in water gradient.

To synthesize the final chemiluminescent probe, oxidation of the enol ether to 1,2-dioxetane was performed. The chemiluminescent precursor (0.02 mmol) was combined with a catalytic amount of methylene blue (~1 mg) in 10 mL of CH_2Cl_2. Oxygen was introduced into the solution while irradiating it with yellow light. Monitoring took place via RP-HPLC. Upon completion, solvent concentration under reduced pressure followed, and further purification was achieved through preparative RP-HPLC using a gradient of CH_3CN in water containing 0.1% TFA. Fractions containing the final product were pooled and subjected to overnight freeze-drying.

Bacterial strains. The laboratory and clinical isolates and ATCC strains used in this study are listed in Table S1.

Limit of detection measurements. *Staphylococcus aureus* ATCC 29213 was cultured in Lysogeny broth at 37°C for 18 hours under aerobic conditions. The initial culture was rinsed with PBS, and the

resulting bacterial pellet was resuspended in 4 mL of PBS to facilitate a 1:5 dilution experiment. For the subsequent procedure, a 96-well plate was utilized, with each well initially loaded with 50□l of the alkaline phosphatase chemiluminescent probe [20□M, 0.1% DMSO], Alkaline phosphatase colorimetric probe [100□M, 0.1% DMSO], or alkaline phosphatase fluorescence probe [20□M, 0.1% DMSO]. Subsequently, 50□l of bacterial aliquot was introduced into each well, marking the commencement of the 1:5 dilution experiment, which was initiated with an OD_{600} of 0.4. The ensuing chemiluminescence signal was monitored over 30 minutes of incubation at 37°C using a Molecular Devices Spectramax i3x. Simultaneously, the fluorescence signal was recorded during the same timeframe at the same temperature using a Tecan Infinite 200 Pro.

Substrate specificity experiments. The specificity of each chemiluminescent probe was assessed in the presence of ten commercially available recombinant enzymes. The chemiluminescent intensity of each probe [10 μM in PBS (pH 7.4), 0.1% DMSO, 37°C] was measured in conjunction with the following commercially available recombinant enzymes: β-glucosidase (from almonds) [10 U/mL], β-glucuronidase (from *E. coli*) [1 U/mL], β-galactosidase (from *E. coli*) [1 U/mL], pyroglutamyl-peptidase I (from *E. coli*) [0.05 mg/mL], alkaline phosphatase (from bovine intestinal mucosa) [1 U/mL], aminopeptidase-M (from Porcine Kidney) [1 U/mL], Nitroreductase (from *E. coli*) [1 mg/mL, 100mM], NADH NQO1 (from *E. coli*) [0.8 mg/mL, 100mM NADH], β-lactamase (from *E. coli*) [2 U/mL], penicillin G-amidase (from *E. coli)* [1 U/mL].

Procedure for Chemiluminescent Measurement of Bacterial Enzymatic Fingerprints. All bacterial strains were cultured in lysogeny broth/brain heart infusion broth at either 37°C or 30°C for 18 hours under aerobic conditions. Subsequently, the initial culture was subjected to a PBS wash, and the bacterial pellet obtained was reconstituted in 4 mL of PBS, aiming for an OD_{600} of 0.8. Following this, a

96-well plate was utilized, and each well was pre-loaded with 50 □l of each chemiluminescent probe [20 □M, 0.1% DMSO]. Next, 50 □l of bacterial aliquot was introduced into each well, bringing the final OD_{600} to 0.4. The resultant chemiluminescence signal was monitored using a Molecular Devices Spectramax iD3 over the course of 1 hour of incubation at 37°C.

Computational methods. The 1-N-N classification method was executed using MATLAB's K-Nearest Neighbors (KNN) algorithm, where K was set to 1, and the Euclidean distance metric was employed for similarity measurement. Furthermore, MATLAB's built-in Principal Component Analysis (PCA) implementation was utilized for visualization, primarily aimed at dimensionality reduction of the dataset. To comprehensively evaluate the efficacy of our approach, the MATLAB KNN classifier was applied to all 4094 potential probe combinations, with K set to 1 and the Euclidean distance metric. This enabled measurement of classification accuracy across all probe combinations, facilitating a robust assessment of the method's performance.

Data acquisition and processing. The data acquisition process involved meticulous aggregation from multiple sources. For each measurement, raw data were gathered by evaluating three distinct wells harboring the target bacteria, contrasted with three control wells that lacked bacteria and served as background references. The processing of these raw data entailed a series of steps. Initially, the mean light intensity value was calculated across measurements from the three wells containing bacteria and similarly for the control wells. Following this, the light intensity was integrated over a one-hour interval in the presence and absence of bacteria. A crucial stage involved subtracting the logarithm of TLE gathered from the control wells (termed "Control") from the logarithm of the TLE gathered from the bacteria-containing wells. To ensure consistency, any negative log ratios were set to zero. This process culminated in the generation of a 12-dimensional vector for each strain, with entries corresponding to the distinct probes in our array.

1-N-N analysis. 1-N-N Analysis computational analysis of data involved the manipulation of 12-dimensional vectors containing background-subtracted log-intensity data. To accomplish this, the K-Nearest Neighbors (KNN) algorithm was employed. Specifically, the MATLAB implementation of KNN was utilized with K set to 1. In congruence with this choice, the Euclidean distance was adopted as the metric to facilitate pairwise comparisons between data points. The KNN algorithm facilitates informed labeling of unknown data points within the test set. This is achieved by assigning to each unknown data point the label of its nearest counterpart within the training set. To ensure the robustness and reliability of outcomes, the dataset of enzymatic profiles underwent a randomized split, resulting in two distinct data sets: the training set encompassing 72% of the data and the test set comprising the remaining 28%. This partitioning strategy is designed to enhance precision and dependability in the classification results for log-intensity data. To guarantee comprehensive coverage and robust evaluation, it is important to note that the partitioning strategy employed also ensures that each bacterium within the dataset is included in both the training and test set, thereby allowing for a thorough assessment of the classification performance. By employing this approach, effective categorization of new data points is achieved through their proximity to reference points within the training set.

Details of the chi-squared (χ^2) resemblance ranking and test.

Definition of the Resemblance Test: The methodology employed in this study focuses on the characterization and classification of bacterial strains based on their enzymatic profiles within a 12-dimensional space. It is grounded in the assumption that these profiles conform to Gaussian distributions. To assess the degree of similarity between an unfamiliar bacterial strain and those cataloged within our dataset, we employ a probability-centered approach. Central to this approach is the Chi-Squared (χ^2) metric, a statistical measure that quantifies deviations from reference statistics and is crucial for evaluating the resemblance of unknown bacteria to those within a reference dataset. The degrees of freedom for the χ^2statistic is set to 12, corresponding to the 12 dimensions of the

enzymatic profile space. This systematic methodology serves as the foundation for probabilistic classification and allows for the identification and categorization of novel bacteria based on their enzymatic profiles.

Data Retrieval: Enzymatic profile data for known bacterial species and the enzymatic profile of an unknown bacterium are retrieved from a structured Excel dataset.

Parameter Extraction: For each known bacterial species, mean vectors and variances are computed to characterize their respective Gaussian distributions. These parameters are pivotal for subsequent analyses.

Calculation of Chi-Squared Statistics: The Chi-Squared statistic is computed by centering and normalizing the mean vectors and variances of the known bacterial species and the unknown bacterium. Careful precautions are taken to prevent division by zero.

Hypothesis Testing: To determine the extent of dissimilarity between the unknown bacterium and the reference species, Chi-Squared statistics and associated p-values are calculated. These p-values are essential for hypothesis testing.

Probabilistic Classification: The Chi-Squared statistics are used to rank the similarity between the unknown bacterium and the reference species. This ranking provides a quantitative measure of resemblance.

Statistical analysis:

Data are presented as means (three or more replicates) ± SD (error bars). All statistical analyses were performed using the two-tailed Student's t-test unless otherwise indicated. Differences were considered significant at $P < 0.05$.

DATA AVAILABILITY

All data supporting the conclusions and findings included in this study are available within the article or Supplementary Information. Any additional information required to reanalyze the data reported in this study is available from the corresponding author upon request.

REFERENCES

1 Maugeri, G., Lychko, I., Sobral, R. & Roque, A. C. A. Identification and Antibiotic-Susceptibility Profiling of Infectious Bacterial Agents: A Review of Current and Future Trends. *Biotechnol. J.* **14**, 1700750 (2019).

2 Berkley, S. Health security's blind spot. *Science* **359**, 1075-1075 (2018).

3 Staub, I. & Sieber, S. A. beta-lactams as selective chemical probes for the in vivo labeling of bacterial enzymes involved in cell wall biosynthesis, antibiotic resistance, and virulence. *J. Am. Chem. Soc.* **130**, 13400-13409 (2008).

4 Wang, Z. M. & Xing, B. G. Small-molecule fluorescent probes: big future for specific bacterial labeling and infection detection. *Chem. Commun.* **58**, 155-170 (2021).

5 Diekema, D. J. & Saubolle, M. A. Clinical Microbiology and Infection Prevention. *J. Clin. Microbiol.* **49**, S57-S60 (2011).

6 Maurer, F. P., Christner, M., Hentschke, M. & Rohde, H. Advances in Rapid Identification and Susceptibility Testing of Bacteria in the Clinical Microbiology Laboratory: Implications for Patient Care and Antimicrobial Stewardship Programs. *Infect. Dis. Rep/* **9**, 6839 (2017).

7 Varadi, L. *et al.* Methods for the detection and identification of pathogenic bacteria: past, present, and future. *Chem. Soc. Rev.* **46**, 4818-4832 (2017).

8 van Dijk, E. L., Auger, H., Jaszczyszyn, Y. & Thermes, C. Ten years of next-generation sequencing technology. *Trends. Genet.* **30**, 418-426 (2014).

9 Tsuchida, S., Umemura, H. & Nakayama, T. Current Status of Matrix-Assisted Laser Desorption/Ionization-Time-of-Flight Mass Spectrometry (MALDI-TOF MS) in Clinical Diagnostic Microbiology. *Molecules* **25**, 4775 (2020).

10 Doern, C. D. & Butler-Wu, S. M. Emerging and Future Applications of Matrix-Assisted Laser Desorption Ionization Time-of-Flight (MALDI-TOF) Mass Spectrometry in the Clinical Microbiology Laboratory A Report of the Association for Molecular Pathology. *J. Mol. Diagn.* **18**, 789-802 (2016).

11 Singhal, N., Kumar, M., Kanaujia, P. K. & Virdi, J. S. MALDI-TOF mass spectrometry: an emerging technology for microbial identification and diagnosis. *Front. Microbiol.* **6**, 791 (2015).

12 Wieser, A., Schneider, L., Jung, J. T. & Schubert, S. MALDI-TOF MS in microbiological diagnostics-identification of microorganisms and beyond (mini review). *Appl. Microbiol. Biot.* **93**, 965-974 (2012).

13 Tan, K. E. *et al.* Prospective Evaluation of a Matrix-Assisted Laser Desorption Ionization-Time of Flight Mass Spectrometry System in a Hospital Clinical Microbiology Laboratory for Identification of Bacteria and Yeasts: a Bench-by-Bench Study for Assessing the Impact on Time to Identification and Cost-Effectiveness. *J. Clin. Microbiol.* **50**, 3301-3308 (2012).

14 Torres-Sangiao, E., Rodriguez, C. L. & Garcia-Riestra, C. Application and Perspectives of MALDI-TOF Mass Spectrometry in Clinical Microbiology Laboratories. *Microorganisms* **9**, 1539 (2021).

15 Franco-Duarte, R. *et al.* Advances in Chemical and Biological Methods to Identify MicroorganismsFrom Past to Present. *Microorganisms* **7**, 130 (2019).

16 Janda, J. M. & Abbott, S. L. Bacterial Identification for Publication: When Is Enough Enough? *J. Clin. Microbiol.* **40**, 1887-1891 (2002).

17 Tien, N. *et al.* Repeated centrifuging and washing concentrates bacterial samples in peritoneal dialysis for optimal culture: an original article. *BMC Microbiol.* **20**, 365 (2020).

18 Amjad, M. An Overview of the Molecular Methods in the Diagnosis of Gastrointestinal Infectious Diseases. *Int. J. Microbiol.* **2020**, 8135724 (2020).

19 Smith, P. B., Tomfohrde, K. M., Rhoden, D. L. & Balows, A. API system: a multitube micromethod for identification of Enterobacteriaceae. *Appl. Microbiol.* **24**, 449-452 (1972).

20 Holmes, B., Willcox, W. R. & Lapage, S. P. Identification of Enterobacteriaceae by the API 20E system. *J. Clin. Pathol.* **31**, 22-30 (1978).

21 Shayegani, M., Maupin, P. S. & McGlynn, D. M. Evaluation of the API 20E system for identification of nonfermentative Gram-negative bacteria. *J. Clin. Microbiol.* **7**, 539-545 (1978).

22 Klingler, J. M. *et al.* Evaluation of the Biolog Automated Microbial Identification System. *Appl. Environ. Microbiol.* **58**, 2089-2092 (1992).

23 Preston-Mafham, J., Boddy, L. & Randerson, P. F. Analysis of microbial community functional diversity using sole-carbon-source utilisation profiles - a critique. *Fems Microbiol. Ecol.* **42**, 1-14 (2002).

24 Roth-Konforti, M. *et al.* Ultrasensitive Detection of Salmonella and Listeria monocytogenes by Small-Molecule Chemiluminescence Probes. *Angew. Chem. Int. Ed.* **58**, 10361-10367 (2019).

25 Babin, B. M. *et al.* Chemiluminescent Protease Probe for Rapid, Sensitive, and Inexpensive Detection of Live Mycobacterium tuberculosis. *ACS Cent. Sci.* **7**, 803-814 (2021).

26 Peukert, C. *et al.* Enzyme-Activated, Chemiluminescent Siderophore-Dioxetane Probes Enable the Selective and Highly Sensitive Detection of Bacterial Pathogens. *Angew. Chem. Int. Ed.* **61**, e202201423 (2022).

27 Aron, A. T. *et al.* In vivo bioluminescence imaging of labile iron accumulation in a murine model of Acinetobacter baumannii infection. *PNAS* **114**, 12669-12674 (2017).

28 Roda, A. & Guardigli, M. Analytical chemiluminescence and bioluminescence: latest achievements and new horizons. *Anal. Bioanal. Chem.* **402**, 69-76 (2012).

29 Ma, C. W. *et al.* Rapid Broad Spectrum Detection of Carbapenemases with a Dual Fluorogenic-Colorimetric Probe. *J. Am. Chem. Soc*. **143**, 6886-6894 (2021).

30 Blau, R., Shelef, O., Shabat, D. & Satchi-Fainaro, R. Chemiluminescent probes in cancer biology. *Nat. Rev. Bioeng.* (2023).

31 Hananya, N. & Shabat, D. Recent Advances and Challenges in Luminescent Imaging: Bright Outlook for Chemiluminescence of Dioxetanes in Water. *ACS Cent. Sci.* **5**, 949-959 (2019).

32 Schaap, A. P., Chen, T. S., Handley, R. S., Desilva, R. & Giri, B. P. Chemical and Enzymatic Triggering of 1,2-Dioxetanes .2. Fluoride-Induced Chemiluminescence from Tert-Butyldimethylsilyloxy-Substituted Dioxetanes. *Tetrahedron Lett.* **28**, 1155-1158 (1987).

33 Green, O. *et al.* Opening a Gateway for Chemiluminescence Cell Imaging: Distinctive Methodology for Design of Bright Chemiluminescent Dioxetane Probes. *ACS Cent. Sci.* **3**, 349-358 (2017).

34 Kagalwala, H. N., Reeves, R. T. & Lippert, A. R. Chemiluminescent spiroadamantane-1,2-dioxetanes: Recent advances in molecular imaging and biomarker detection. *Curr. Opin. Chem. Biol.* **68**, 102134 (2022).

35 Kagalwala, H. N., Gerberich, J., Smith, C. J., Mason, R. P. & Lippert, A. R. Chemiluminescent 1,2-Dioxetane Iridium Complexes for Near-Infrared Oxygen Sensing. *Angew. Chem. Int. Ed.* **61**, e202115704 (2022).

36 Chen, C. *et al.* Amplification of Activated Near-Infrared Afterglow Luminescence by Introducing Twisted Molecular Geometry for Understanding Neutrophil-Involved Diseases. *J. Am. Chem. Soc.* **144**, 3429-3441 (2022).

37 Shelef, O. *et al.* Turn on chemiluminescence-based probes for monitoring tyrosinase activity in conjunction with biological thiols. *Chem. Commun.* **57**, 11386-11389 (2021).

38 Scott, J. I. *et al.* A Functional Chemiluminescent Probe for in Vivo Imaging of Natural Killer Cell Activity Against Tumours. *Angew. Chem. Int. Ed.* **60**, 5699-5703 (2021).

39 Huang, J. S., Jiang, Y. Y., Li, J. C., Huang, J. G. & Pu, K. Y. Molecular Chemiluminescent Probes with a Very Long Near-Infrared Emission Wavelength for in Vivo Imaging. *Angew. Chem. Int. Ed.* **60**, 3999-4003 (2021).

40 Haris, U., Kagalwala, H. N., Kim, Y. L. & Lippert, A. R. Seeking Illumination: The Path to Chemiluminescent 1,2-Dioxetanes for Quantitative Measurements and In Vivo Imaging. *Acc. Chem. Res.* **54**, 2844-2857 (2021).

41 Ye, S. *et al.* A Highly Selective and Sensitive Chemiluminescent Probe for Real-Time Monitoring of Hydrogen Peroxide in Cells and Animals. *Angew. Chem. Int. Ed.* **59**, 14326-14330 (2020).

42 Huang, J. S., Huang, J. G., Cheng, P. H., Jiang, Y. Y. & Pu, K. Y. Near-Infrared Chemiluminescent Reporters for In Vivo Imaging of Reactive Oxygen and Nitrogen Species in Kidneys. *Adv. Funct. Mater.* **30**, 2003628 (2020).

43 Gutkin, S., Green, O., Raviv, G., Shabat, D. & Portnoy, O. Powerful Chemiluminescence Probe for Rapid Detection of Prostate Specific Antigen Proteolytic Activity: Forensic Identification of Human Semen. *Bioconjug. Chem.* **31**, 2488-2493 (2020).

44 Shelef, O. *et al.* Ultrasensitive chemiluminescent neuraminidase probe for rapid screening and identification of small-molecules with antiviral activity against influenza A virus in mammalian cells. *Chem. Sci.* **13**, 12348-12357 (2022).

45 Yoon, S. A., Park, S. Y., Cha, Y. J., Gopala, L. & Lee, M. H. Strategies of Detecting Bacteria Using Fluorescence-Based Dyes. *Front. Chem*. **9**, 743923 (2021).

46 Orenga, S., James, A. L., Manafi, M., Perry, J. D. & Pincus, D. H. Enzymatic substrates in microbiology. *J. Microbiol. Meth.* **79**, 139-155 (2009).

47 Bergey, D. H., Krieg, N. R. & Holt, J. G. *Bergey's manual of systematic bacteriology*. (Williams & Wilkin*s,* Baltimore*,* 1984).

48 Mulani, M. S., Kamble, E. E., Kumkar, S. N., Tawre, M. S. & Pardesi, K. R. Emerging Strategies to Combat ESKAPE Pathogens in the Era of Antimicrobial Resistance: A Review. *Front. Microbiol.* **10**, 539 (2019).

49 Cover, T. M. & Hart, P. E. Nearest Neighbor Pattern Classification. *IEEE Trans. Inf. Theory* **13**, 21-27 (1967).

50 James, A. L. & Yeoman, P. Detection of Specific Bacterial Enzymes by High Contrast Metal Chelate Formation .2. Specific Detection of Escherichia-Coli on Multipoint-Inoculated Plates Using 8-Hydroxyquinoline-Beta-D-Glucuronide. Zentralbl. Bakteriol. Mikrobiol. Hyg. **267**, 316-321 (1988).

51 Avire, N. J., Whiley, H. & Ross, K. A Review of Streptococcus pyogenes: Public Health Risk Factors, Prevention and Control. *Pathogens* **10**, 248 (2021).

52 Murray, P. R., Wold, A. D., Schreck, C. A. & Washington, J. A., II. Effects of selective media and atmosphere of incubation on the isolation of group A streptococci. *J. Clin. Microbiol.* **4**, 54-56 (1976).

53 Schulthess, B. *et al.* Identification of Gram-positive cocci by use of matrix-assisted laser desorption ionization-time of flight mass spectrometry: comparison of different preparation methods and implementation of a practical algorithm for routine diagnostics. *J. Clin. Microbiol.* **51**, 1834-1840 (2013).

54 Anderson, N. W. *et al.* Multicenter Clinical Evaluation of the illumigene Group A Streptococcus DNA Amplification Assay for Detection of Group A Streptococcus from Pharyngeal Swabs. *J. Clin. Microbiol.* **51**, 1474-1477 (2013).

55 Cellier, M. *et al.* Novel chromogenic aminopeptidase substrates for the detection and identification of clinically important microorganisms. *Bioorganic. Med. Chem.* **22**, 5249-5269 (2014).

ACKNOWLEDGMENTS

This work was supported by funding from the Israel Ministry of Science Technology # 0004857 (DS and MF). S.R. acknowledges support from the European Research Council (ERC) under the European Union's Horizon 2020 research and innovation program (grant agreement No. 947731). O.S. acknowledges support from the Adams Fellowship Program of the Israel Academy of Science and

Humanities. M.A. acknowledges the discussion with Ulysse Mizrahi. M.J-K acknowledges support from the Israeli Ministry of Science, Technology & Space for the Levi Eshkol Scholarship (Scholarship 315461).

AUTHOR INFORMATION

Authors and Affiliations

School of Chemistry, Raymond & Beverly Sackler Faculty of Exact Sciences, Tel Aviv University, Tel Aviv, 6997801, Israel.

Contributions

M.F., D.S., and S.R. directed this research. O.S., T.K., and R.T. conducted laboratory experiments. M.A. performed the computational analysis with the guidance of S.R. T.K., M.J-K. implemented bacterial methodology with the guidance of M.F. R.T. and O.S. synthesized the chemical compounds with the guidance of D.S. M.F. conceived the project and wrote the paper. All authors discussed and reviewed the final manuscript.

Corresponding authors

Correspondence to Shlomi Reuveni, Doron Shabat, or Micha Fridman.

ETHICS DECLARATIONS

Competing interests

The authors declare no competing interests.